INSTITUTE OF PHYSICS PUBLISHING JOURNAL OF PHYSICS B: ATOMIC, MOLECULAR AND OPTICAL PHYSICS

J. Phys. B: At. Mol. Opt. Phys. **39** (2006) L9–L16 doi:10.1088/0953-4075/39/1/L02

LETTER TO THE EDITOR

Partial photoionization cross sections of doubly excited helium below the ionization thresholds I_8 and I_9

Y H Jiang[1,2], R Püttner[1], R Hentges[3], J Viefhaus[3], M Poygin[1], C Cacho[4], U Becker[3], J M Rost[2] and G Kaindl[1]

[1] Institut für Experimentalphysik, Freie Universität Berlin, Arnimallee 14, D-14195 Berlin-Dahlem, Germany
[2] Max-Planck-Institut für Physik Komplexer Systeme, Nöthnitzer Strasse 38, D-01187 Dresden, Germany
[3] Fritz-Haber-Institut Berlin, Faradayweg 4-6, D-14195 Berlin-Dahlem, Germany
[4] CCLRC Daresbury Laboratory, Warrington, Cheshire WA4 4AD, UK

Received 14 September 2005, in final form 15 November 2005
Published 5 December 2005
Online at stacks.iop.org/JPhysB/39/L9

Abstract

Partial photoionization cross sections (PCSs), σ_n, leading to final states of singly ionized helium, $He^+(n)$, were measured in the region of doubly excited helium below the ionization thresholds I_8 and I_9. The experiments were performed at BESSY II at high photon resolution, $\Delta E \cong 6$ meV, using a time-of-flight electron spectrometer. A comparison with recent eigenchannel R-matrix calculations reveals good agreement. The results of these measurements underline previous studies on quantum chaos in helium, which were mainly based on theoretical results. They also allow a critical assessment of the theoretical methods that produce the data used for a statistical analysis of double-excitation states with respect to quantum chaos, which is expected to occur very close to the double-ionization threshold. PCSs provide additional information to that derivable from total cross sections (TCSs). In the present PCS spectra, the resonance $8, 4_{10}$ of the secondary series, which could not be resolved in the TCS, is clearly observed.

1. Introduction

Ever since their first observation by Madden and Codling in 1963 [1], double-excitation states in helium are considered as prototypical examples of two-electron systems with strong electron correlation. The observation by Madden and Codling that the various Rydberg series have considerably different intensities could not be explained in an independent electron picture and resulted in the introduction of new approximate quantum numbers N, $K_{n'}$ [2, 3]. Here, N (n') is the principal quantum number for the inner (outer) electron and K an angular-correlation quantum number that reflects the angle between the two electrons and the nucleus. Subsequently, it was shown that these approximate quantum numbers are identical to those exact quantum numbers which describe the separable two-centre Coulomb problem of

H_2^+ [4]. In the last four decades, these doubly excited states of helium were studied intensively by photon excitation [5–7] and charged particle [8–10] impact. The latter work, based on the impact of electrons [8, 9], protons [8, 10] or other excited charged particles, like C^{q+} and F^{q+} [8], allows us to study doubly excited states such as $2s^2(^1S)$ or $2p^2(^1D)$, which are not accessible within the dipole approximation. However, charged-particle excitation provides only relatively low energy resolution and is, therefore, limited to the low-energy region with the inner electron in the $N = 2$ shell. In contrast, photon impact studies are strictly limited to $^1P^o$ final states by the dipole selection rule but can be carried out with very high energy resolution up to $\Delta E \cong 1$ meV [5]. For this reason, photon impact excitation is better suited for studies in the energy region close to the higher single ionization thresholds (SITs), I_N [6, 7]; here, I_N stands for the SIT of the Rydberg series N, $K_{n'}$, with $n' \to \infty$.

In the energy region close to the double-ionization threshold, interferences due to the overlap of perturbers from various Rydberg series with different N render the excitation spectra rather complicated [6, 7]. In this case, all spectral profiles of a resonance, including its position, linewidth, Fano q parameter and intensity, will be modulated. As a result, the approximate quantum numbers N and K are expected to lose their meaning, and the regularities in the two-electron resonance spectrum start to dissolve, particularly in the region very close to double-ionization threshold, where quantum chaos is expected to occur [11]. The statistical analysis of the spacings between neighbouring resonances in the total cross sections (TCSs), σ_T, below the SIT I_9 of He^+ has already revealed a transition towards quantum chaos [12]. In this transition region, a partial loss of meaning of the quantum number N has been found, where K remains approximately a good quantum number, for K close to $K_{max} = N - 1$. Since $K \cong -N\langle\cos\Theta\rangle$, where Θ is the angle from the nucleus to the two electrons, Θ approaches π for $K \cong N$. Therefore, the Rydberg series with $K = N - 2$ and $N - 4$, which are visible in the experimental spectra, can be related to classical periodic orbits of a collinear eZe configuration with the two electrons on opposite sides of the nucleus. It is well known in classical dynamics that the eZe configuration can be strongly chaotic in the radial direction but stable in the angular direction [11]. In this way, classical dynamics explains the stability of K and the loss of N as a good quantum number. The loss of N can also be understood by the increasing number of perturbers that strongly influence the energy positions of the resonances. The validity of K as a good quantum number is tantamount to the fact that the spectra are dominated by the principal series N, $(N-2)_{n'}$ since $K = N - 2$ carries most of the intensity. It should be mentioned here that very recently state-of-the-art complex rotation calculations for the TCS of three-dimensional helium have reached the SIT I_{17} [13]; the results were confirmed in a remarkable way up to I_{15} by recent experimental data [14]. A preliminary statistical analysis of these new data revealed interesting precursor signatures of quantum chaos in doubly excited helium.

Since various outgoing channels may couple, the partial cross sections (PCSs), σ_n, are more sensitive to the theoretical methods and the quality of the wavefunctions applied than the TCS, σ_T. Here, σ_n are the PCSs for the outgoing channels that lead to $He^+(n)$, with the remaining single electron in a state with principal quantum number n. σ_n are also more sensitive to influences of perturbers because each decay channel can be influenced in a different way. As a result, more resonances with pronounced variations are expected in σ_n in comparison to σ_T. As an illustration, the resonance $8, 4_{10}$ of the secondary series was resolved in PCS measurements in the present work, while in TCS studies this resonance could not yet be observed [6].

In this way, experimental studies of PCSs, σ_n, can substantiate theoretical methods and assure the validity of statistical analysis focusing on quantum chaos. Since the signatures of quantum chaos are expected to show up particularly clearly very close to the double-

ionization threshold of He, the last eV below this threshold has drawn considerable attention, both in experimental and in theoretical studies. So far, however, these studies have been restricted mainly to TCSs [6, 12–16]. First measurements of PCSs were performed by Lindle *et al* [17]; due to the low photon intensities achieved at that time at first-generation light sources, these measurements were limited to excitations below the SIT I_3. Menzel *et al* were the first to report on measurements of PCSs up to the SIT I_5 employing two spherical-sector-plate electrostatic analysers [18, 19]. In the last year, we extended the experimental studies of PCSs up to the SIT I_7 [20], whereas Czasch *et al* [21] studied the photon energy region from the SIT I_9 to I_{16}. Recent calculations were performed by Schneider *et al* [22] and van der Hart and Greene [23], who reported theoretical data for σ_n up to the SIT I_9.

In the present letter, we report on experimental results for PCSs in the region of doubly excited helium up to the SITs I_8 and I_9 of He^+, and in this way, we shall fill the gap between our previous measurements [20] and the experimental results reported by Czasch *et al* [21]. Along with the experimental data, the results of state-of-the-art *R*-matrix calculations are presented.

2. Experimental setup and procedure

State-of-the-art high-resolution monochromators in combination with time-of-flight (TOF) photoelectron spectrometers allow us to explore the autoionization decay of resonances in the region close to the double-ionization threshold of helium. Here, we present photoemission measurements for states below the SITs I_8 and I_9 and extract the various PCSs from the recorded photoelectron spectra in this energy region. The experiments were performed at the undulator beamline U125/2-SGM (BUS-beamline) [24] of the Berliner Elektronenspeicherring für Synchrotronstrahlung (BESSY) using a photon energy resolution of $\cong$6 meV (FWHM). The TOF spectrometer [25] was mounted at the magic angle, i.e. in the dipole plane perpendicular to the incoming photon beam at an angle of $\theta = 55^\circ$ relative to the polarization direction of the linearly polarized incoming light. In this geometry, the angular distribution can be assumed to cause no effects. A needle (10 cm long, with an inner diameter of less than 500 μm) directs an effusive jet of gas to the interaction region; the He background pressure in the chamber was $\cong 10^{-4}$ mbar. From the count rates and the calculated cross sections, we estimated the He pressure in the interaction region to be of the order of 10^{-2} mbar. TOF photoelectron spectra were taken for each photon energy and converted into photoemission spectra by a time-to-energy conversion procedure.

In order to eliminate influences caused by the decrease of the ring current and the fluctuations of the gas pressure in the interaction region during data taking, the spectra were normalized to the intensity of the $n = 1$ photoemission line, i.e. the PCS σ_1 was assumed to be without structure. Based on theoretical results, which show some weak resonances in σ_1 (see figures 1 and 2), we can estimate that the error bars of this procedure are $\leqslant 3\%$ for measurements below the SIT I_8 and $\leqslant 2\%$ below I_9. Photon energies were calibrated by adjustment to theoretical results [16].

3. Theoretical method

The eigenchannel *R*-matrix method [26], combined with a close-coupling scheme [27], was employed for calculating PCSs. The configuration space is partitioned into the reaction region (defined by $r_i < r_0$, where r_i are the electron distances from the nucleus) and the external region ($r_i > r_0$). In the reaction region, the full two-electron problem can be solved numerically by bound-state configuration interaction techniques to obtain the

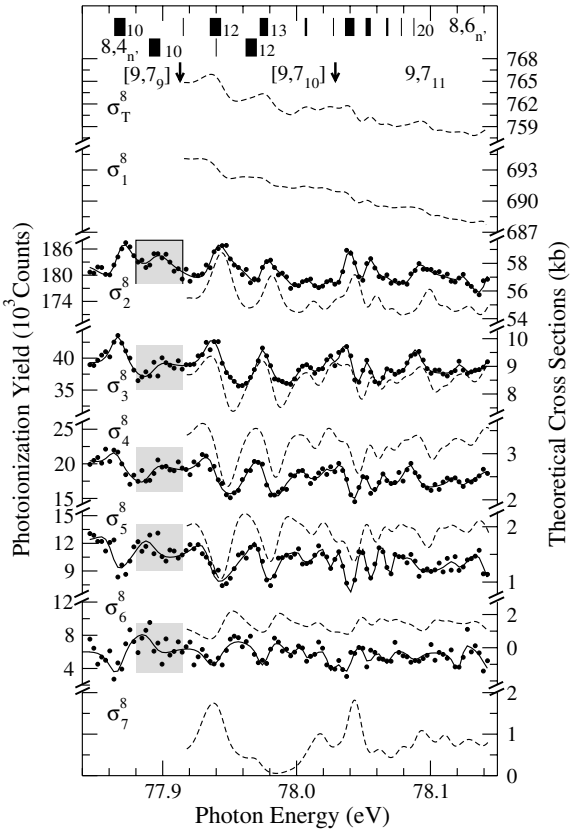

Figure 1. Experimental partial cross sections, σ_n^8, leading to the final states $He^+(n)$,with $n = 2$–6, along with the results of the eigenchannel R-matrix calculations. The data were taken in the photon energy region between 77.84 eV and 78.15 eV. The two vertical-bar diagrams in the upper part of the figure give the assignments of the double-excitation resonances by specifying n'; the widths of bars are proportional to the linewidths of the corresponding resonances [12]. The vertical arrows mark the calculated energies of the perturbers $[9, 7_9]$ and $[9, 7_{10}]$. The energy position of resonance $8, 4_{10}$ of the secondary series is marked by grey bars. The data points are the present experimental results, with the solid curves through the data points representing the fit results. The dashed curves represent the results of the R-matrix calculations convoluted with a Gaussian of 6 meV width (FWHM) to simulate finite experimental resolution.

so-called eigenchannel wavefunctions. These wavefunctions are linearly combined into helium wavefunctions of experimentally observed channels. In the external region, a multichannel wavefunction, with one bound and one continuum wavefunction, is again linearly combined into a helium eigenfunction according to the incoming-wave boundary condition [27]. By matching the linear combinations of the multichannel basis functions for the two regions, one can determine an accurate final-state wavefunction $\Psi_f^{(-)}$, which describes the experimentally observed channel f. The PCS for absorbing a photon of energy $h\nu$ from the initial state Ψ_0 (here the ground state of helium) reads [28]

$$\sigma_f = \frac{8\pi^3\nu}{c}\left|\left\langle\Psi_f^{(-)}\right|D|\Psi_0\right\rangle\right|^2, \tag{1}$$

with the dipole operator D and the speed of light c. For the results presented here, a radius of $r_0 = 200$ au was used and a total of 1080 closed-type (i.e., zero at the radius r_0) and 20

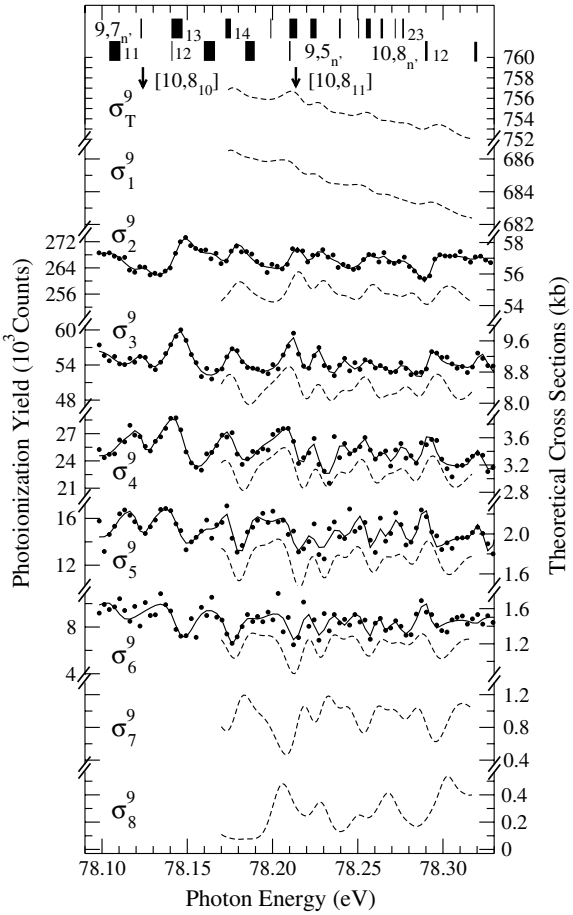

Figure 2. Experimental partial cross sections, σ_n^9, leading to the final states $He^+(n)$, with $n = 2$–6, respectively, in the energy region from 78.09 eV to 78.33 eV, along with the results of the eigenchannel R-matrix calculations; for details, see the caption of figure 1.

open-type (i.e., non-zero at the radius r_0) one-electron wavefunctions, with orbital angular momenta up to 9, were included. 9610 closed-type two-electron configurations were included in the calculation of the final-state wavefunctions. For each channel, in which one electron can escape from the reaction region, two open-type orbitals for the outer electron were included in addition to the closed-type basis set [22].

4. Experimental results and discussion

The resonance profiles in the TCS can be described by the Fano formula [29]

$$\sigma(E) = \sigma_a \frac{(q+\epsilon)^2}{1+\epsilon^2} + \sigma_b \qquad \text{with} \qquad \epsilon = 2\frac{E - E_r}{\Gamma}. \tag{2}$$

Here, E_r is the resonance energy and Γ the natural width that is determined by the decay rate of the resonance, representing the discrete/continuum mixing strength. The Fano parameter q represents the ratio of the dipole matrix element of a transition to a discrete state to that of a transition to the continuum, which interacts with the discrete state. σ_a and σ_b represent

non-resonant background cross sections for transitions to continuum states that interact or do not interact with discrete autoionization states, respectively [29]. Note that the Fano formula, which had been developed for describing the lineshapes of resonances in the TCS, has the same mathematical structure as the exact formula given by Starace for describing the resonances in the PCS [30]. As a consequence, it is possible to describe the PCSs by the Fano formula, but in this case q represents only an effective parameter without deeper meaning. In analysing our data, we fitted the various PCSs for a given energy region by the Fano formula in a least-squares fit procedure using a single Gaussian to simulate the experimental resolution function. In this way, σ_n leading to different final states of $He^+(n)$ were fitted to equation (2) with the fixed energy position E_r and linewidth Γ, which were taken from the calculations used for the statistical analysis in [12], but free parameters q and intensity. An additional parameter was used for the position shift of whole spectra between the experiment and the theory. The results of this fit procedure are given as solid curves through the data points in figures 1 and 2. This simple fit approach shows good agreement with the experimental results and clearly confirms the theoretical data used for the statistical analysis on the nearest-neighbour spacing that revealed a transition towards quantum chaos [12]. Although the previously unobserved resonance $8, 4_{10}$ of the secondary series could be observed, the fits still show that the PCSs are dominated by the resonances of the principal series N, $(N-2)_{n'}$. This can be understood with K being still an approximate quantum number, as has been observed with the TCS [12]. In summary, the present fit results are fully in line with previous findings of [12] on quantum chaos.

Note that for convenience we employ in our discussion the notation σ_n^N to label the PCSs which represent the decays to the ionized final state, $He^+(n)$, with possible decay channels $n = 1, 2, 3, \ldots, N-1$ below the SIT I_N. Figures 1 and 2 display the results of the present work for the PCSs σ_n^8 and σ_n^9 (with $n = 2$–6), along with the results of the least-squares-fit analysis (filled data points and solid curves), respectively. The results for the PCSs as well as the TCS of the eigenchannel R-matrix calculations are convoluted with the present monochromator resolution of $\cong$6 meV (FWHM) and presented in form of the dashed lines in these two figures. The calculated TCS and PCSs are given in kb on the right coordinate axis. One can see that the variations in the PCSs, σ_n^N, caused by the resonances, increase relative to the constant background with increasing quantum number n. The energy positions of the perturbers $[9, 7_9]$, $[9, 7_{10}]$, $[10, 8_{10}]$ and $[10, 8_{11}]$ are marked by vertical arrows in figures 1 and 2. In general, there is good agreement for the variations in the lineshapes, amplitudes and relative positions of the resonances between the experimental and the theoretical spectra.

Energy position and width of resonance $8, 4_{10}$ of the secondary series are marked by grey bars in the spectra of figure 1; this energy region is shown in more detail together with resonance $8, 6_{10}$ in figure 3. The previously reported total cross section [6] in this energy region is also plotted in figure 3(a). Although the data for the TCS have good statistics and were recorded with high resolution ($\cong$4 meV), resonance $8, 4_{10}$ is absent in the TCS spectrum. In contrast, it is clearly observed in all decay channels below the SIT I_8 (see figures 3(b)–(f)). The suppression of resonance $8, 4_{10}$ in the TCS data is due to the fact that resonance $8, 4_{10}$ exhibits quite different lineshapes in the PCSs, which cancel out in the TCS. These different lineshapes are due to different couplings to various σ_n. In figure 3(f), the signal-to-noise ratio is lowest and traces of resonance $8, 4_{10}$ can only be identified by curve fitting of the σ_6^8 data.

Statistical error bars in the PCS spectra were estimated to be $\leqslant$1% (for σ_2^8 and σ_2^9), 1% (for σ_3^8 and σ_3^9), 3% (for σ_4^8), 2% (for σ_4^9), 6% (for σ_5^8), 4% (for σ_5^9), 11% (for σ_6^8) and 7% (for σ_6^9). Note that possible systematic fluctuations caused by normalizing the spectra to σ_1 were not taken into account in these numbers. An increase of the error bars in σ_n with increasing n can

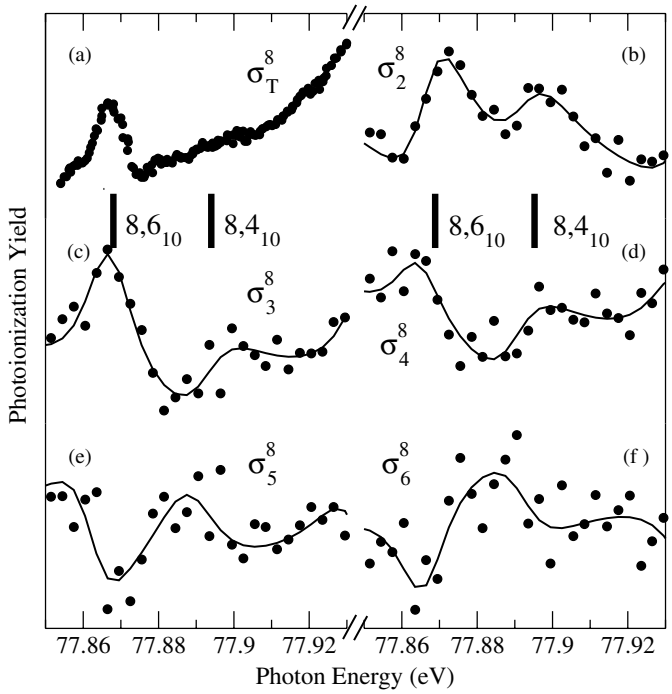

Figure 3. Experimental partial cross sections σ_n^8 for resonances $8, 6_{10}$ and $8, 4_{10}$ in the energy region from 77.85 eV to 77.93 eV. (a) Previous total cross section [6]; results of the present work for (b) σ_2^8, (c) σ_3^8, (d) σ_4^8, (e) σ_5^8 and (f) σ_6^8. The solid lines through the data points represent the fit results.

readily be understood by taking into account that (i) the lower decay channels are characterized by larger cross sections, and (ii) the corresponding photoelectrons have higher kinetic energies that are detected with higher efficiency (through higher transmission) in the TOF spectrometer. Both facts give rise to higher count rates and therefore to smaller error bars, consistent with our previous observations below the SIT I_7 [20]. The PCSs σ_7^8, σ_7^9 and σ_8^9 could not be obtained from the present measurements due to small PCSs and the relatively low transmission of the TOF spectrometer for very slow electrons. Theoretical results for σ_T^8, σ_1^8, σ_2^8, σ_3^8 and σ_4^8 are presented here for the first time. Note that theoretical cross sections have been shifted in figure 1 by 12 meV and in figure 2 by 10 meV to higher energies to better fit the experimental data. These shifts are almost the same as those reported previously for the PCSs below the SIT I_7 [20].

5. Conclusions

In the present work, the PCSs σ_n^8 and σ_n^9 were measured in the energy regions below the SITs I_8 and I_9, respectively, and compared with the results of eigenchannel R-matrix calculation. In general, the experimental data agree well with the theoretical results. The resonance $8, 4_{10}$, which is unresolved in the TCS data, could be clearly resolved in the present channel-resolved measurements. The fits of the present PCSs are a further confirmation of the energy positions used for the statistical analysis of the nearest-neighbour spacing as well as the validity of K as a good quantum number and, therefore, present, in summary, a further confirmation of the

studies on quantum chaos mainly based on theoretical results given in [12]. These results show that experimental PCS, σ_n, represent critical tests for future theoretical results in the energy region above I_9. This is important in the sense that these theoretical results in turn produce directly the resonance parameters that can be employed for a statistical analysis of double-excitation states in the energy region extremely close to double-ionization threshold, with the aim to examine the helium atom for the signatures of quantum chaos.

Acknowledgments

This work was supported by the Bundesministerium für Bildung und Forschung, project no 05 KS1EB1/2, and the Deutsche Forschnungsgemeinschaft, project no PU 180/2-1. The input by C-N Liu and T Schneider at the early stages of this work is gratefully acknowledged. YHJ thanks the MPI für Physik Komplexer Systeme, Dresden, for a two-year research fellowship.

References

[1] Madden R P and Codling K 1963 *Phys. Rev. Lett.* **10** 516
[2] Herrick D R and Sinanoğlu O 1975 *Phys. Rev.* A **11** 97
[3] Lin C D 1984 *Phys. Rev.* A **29** 1019
[4] Feagin J M and Briggs J S 1986 *Phys. Rev. Lett.* **57** 984
[5] Schulz K, Kaindl G, Domke M, Bozek J D, Heimann P A, Schlachter A S and Rost J M 1996 *Phys. Rev. Lett.* **77** 3086
[6] Domke M, Schulz K, Remmers G, Kaindl G and Wintgen D 1996 *Phys. Rev.* A **53** 1424
[7] Püttner R, Domke M, Grémaud B, Martins M, Schlachter A S and Kaindl G 1996 *J. Electron Spectrosc. Relat. Phenom.* **53** 1424
[8] Giese J P, Schulz M, Swenson J K, Schöne , Benhenni M, Varghese S L, Vane C R, Dittner P F, Schafroth S M and Datz S 1990 *Phys. Rev.* A **42** 1231
[9] Liu X, Zhu L, Yuan Zh, Li W, Cheng H, Huang Y, Zhong Zh, Xu K and Li J 2003 *Phys. Rev. Lett.* **91** 193203
[10] Htwe W T, Vajnai T, Barnhart M, Gaus A D and Schulz M 1994 *Phys. Rev. Lett.* **73** 1348
[11] Tanner G, Richter K and Rost J M 2000 *Rev. Mod. Phys.* **72** 497
[12] Püttner R, Grémaud B, Delande D, Domke M, Martins M, Schlachter A S and Kaindl G 2001 *Phys. Rev. Lett.* **86** 3747
[13] Delande D 2005 unpublished
[14] Jiang Y H, Püttner R, Martins M and Kaindl G 2005 unpublished
[15] Rost J M, Schulz K, Domke M and Kaindl G 1997 *J. Phys. B: At. Mol. Opt. Phys.* **30** 4663
[16] Grémaud B and Delande D 1997 *Europhys. Lett.* **40** 363
[17] Lindle D W, Ferrett T A, Becker U, Kobrin P H, Truesdale C M, Kerkhoff H G and Shirley D A 1985 *Phys. Rev.* A **31** 714
[18] Menzel A, Frigo S P, Whitfield S B, Caldwell C D, Krause M O, Tang J Z and Shimamura I 1995 *Phys. Rev. Lett.* **75** 1479
[19] Menzel A, Frigo S P, Whitfield S B, Caldwell C D and Krause M O 1996 *Phys. Rev.* A **54** 2080
[20] Jiang Y H, Püttner R, Hentges R, Viefhaus J, Poiguine M, Becker U, Rost J M and Kaindl G 2004 *Phys. Rev.* A **69** 042706
[21] Czasch A *et al* 2004 *Phys. Scr.* **110** 141
[22] Schneider T, Liu Ch N and Rost J M 2002 *Phys. Rev.* A **65** 042715
[23] van der Hart H W and Greene C H 2002 *Phys. Rev.* A **66** 022710
[24] Martins M, Kaindl G and Schwentner N 1999 *J. Electron Spectrosc. Relat. Phenom.* **101** 965
[25] Becker U, Szostak D, Kerkhoff H G, Kupsch M, Langer B, Wehlitz R, Yagishita A and Hayaishi T 1989 *Phys. Rev.* A **39** 3902
[26] O'Mahony P F and Greene C H 1985 *Phys. Rev.* A **31** 250
[27] Pan C, Starace A F and Greene C H 1996 *Phys. Rev.* A **53** 840
[28] Starace A F 1982 *Handbuch der Physik: Corpuscles and Radiation in Matter* vol 31 ed W Mehlhorn (Berlin: Springer)
[29] Fano U and Cooper J W 1965 *Phys. Rev.* A **137** 1364
[30] Starace A F 1977 *Phys. Rev.* A **16** 231